Programming and Numerical Analysis of a Honeycomb Structure to Obtain Mechanical Properties with Different Cases When Load Is Applied

K. ATHUL AJAYAN[1], DR. J. SURESH KUMAR[2], DR. SATISH BABU[3]
[1]PG Scholar, Dept of Mechanical, JNTU College of Engineering and Technology Mou CITD, Hyderabad, TS, India.
[2]Professor, Dept of Mechanical, JNTU College of Engineering and Technology, Hydrabad, TS, India.
[3]Professor, Dept of Mechanical, JNTU College of Engineering and Technology, Hydrabad, TS, India.

Abstract: This research is on theoretical analysis of the hexagonal honeycomb cells by changing the angles of the cell from ($25^{\circ}$to 40°) and also the thickness of the cell from (1mm to 2mm). Numerical analysis can be done by using analytical equations for stress and energy, by taking hardness and plastic collapse of the honeycomb structure. The validation is done by the acquired numerical results and the simulation done in MATLAB. In order to validate the numerical analysis in MATLAB a simulation test has been done in ANSYS software. The stress-strain diagram has achieved and compared with the obtained numerical values. The obtained numerical value has very less difference when compared to the simulation test done in ANSYS.

Keywords*:* Hexagonal Honeycomb Structure, Strain Energy, Plastic Collapse, Energy Absorption.

I. INTRODUCTION

Aluminum honeycomb structures are well known energy absorbers and have wide applications in automobiles, aircrafts and packaging industries. Tensile and compression tests on each row are performed on material properties. The validation and comparison of acquired analytical equations and energy absorption of the honeycomb structure which is made of aluminum is simulated in MATLAB. In order to validate the numerical simulation method in MATLAB, an Analytical test has been conducted in Ansys software with different weight and with low velocity on a honeycomb structure. In analysis over the honeycomb structural will analyzed based on the shape and structural with dynamic and static loads. in analysis the explicit dynamic will done to find the strength and weakness of the structural and in static we can determine the life and safety factor of the honeycomb by single or double layers. The challenge to the materials community in the coming decade is, quite simply, to provide the materials necessary to achieve the extraordinary goals set forth by the aerospace community. Honeycomb sandwich construction has been an integral part of airplane design and construction for many years. Common applications today include aluminum-based honeycomb panels used as lightweight and stiff flooring material in commercial airliners and as noise-attenuating ring sections in jet engine nacelles. The mechanical properties of honeycomb panels of interest to designers are generally specified as tensile or compressive strength and modulus, and shear strength and modulus. Tensile or compressive strength is the ultimate tensile or compressive strength of the honeycomb panel when measured in the short transverse direction. The sandwiched Honeycomb structure makes it strong, and the light weight makes the aircraft more fuel efficient. But these honeycomb structures are very bad at blocking low-frequency noise - like the noise of an aircraft engine. And adding insulation materials to limit the noise would add significant weight to the aircraft, making it much less fuel efficient, honeycomb structure creating an extremely fire resistant, lightweight, stiff, and strong sandwich core. However, this core alone is not strong enough. Although often lighter and stronger than similar aluminum aircraft components, composite sandwich panels are still susceptible to damage. Below is a side view of a typical for flap. Notice how the honeycomb core is curved with the skin and the majority of the internal area is hollow. The plastic collapse loads corresponding to various failure mechanisms are obtained by equating the internal work at the plastic hinges to the external work by loads during the virtual displacement. This requires evaluation of displacements and plastic hinge rotations. As the plastic deformations at collapse are considerably larger than elastic ones, it is assumed that the frame remains rigid between supports and hinge positions i.e. all plastic rotation occurs at the plastic hinges. Plastic analysis is based on the idealization of the stress-strain curve as elastic-perfectly-plastic. It is further assumed that the width-thickness ratio of plate elements is small so that local buckling does not occur- in other words the sections will classify as plastic. With these assumptions, it can be said that the section will reach its plastic moment capacity and then undergo considerable rotation at this moment. With these assumptions, we will now look at the behavior of a beam up to collapse.

Dynamic compression behaviors of density-homogeneous and density-graded irregular honeycombs are investigated using cell-based finite element models under a constant-velocity impact scenario. A method based on the cross-sectional engineering stress is developed to obtain the one-dimensional stress distribution along the loading direction in a cellular specimen. The cross-sectional engineering stress is contributed by two parts: the node-transitive stress and the contact-induced stress, which are caused by the nodal force and the contact of cell walls, respectively. It is found that the contact-induced stress is dominant for the significantly enhanced stress behind the shock front. The stress enhancement and the compaction wave propagation can be

observed through the stress distributions in honeycombs under high-velocity compression. The single and double compaction wave modes are observed directly from the stress distributions.

II. IN-PLANE PROPERTIES

We are assuming that t/l is small this also means that the relative density is small we are able to neglect axial and shear deformation. Deformation is small and I am going to neglect any changes in the geometry of the cell. The cell wall is linear elastic isotropic. Honeycomb is orthotropic structure remains the same when it is related 180° about each of three mutually perpendicular axis. In the case of an orthotropic material, the number of independent elastic constants is reduced to nine, as various stiffness and compliance terms are interrelated. This is clearly seen when the reference system of coordinates is selected along principal planes of materials symmetry, that is, in case of a specially orthotropic material.

$$\begin{bmatrix}\sigma_1\\ \sigma_2\\ \sigma_3\\ \tau_4\\ \tau_5\\ \tau_6\end{bmatrix} = \begin{bmatrix}C_{11} & C_{12} & C_{13} & 0 & 0 & 0\\ C_{21} & C_{22} & C_{23} & 0 & 0 & 0\\ C_{31} & C_{32} & C_{33} & 0 & 0 & 0\\ 0 & 0 & 0 & C_{44} & 0 & 0\\ 0 & 0 & 0 & 0 & C_{55} & 0\\ 0 & 0 & 0 & 0 & 0 & C_{66}\end{bmatrix}\begin{bmatrix}\varepsilon_1\\ \varepsilon_2\\ \varepsilon_3\\ \gamma_4\\ \gamma_5\\ \gamma_6\end{bmatrix} \& \quad (1)$$

$$\begin{bmatrix}\varepsilon_1\\ \varepsilon_2\\ \varepsilon_3\\ \gamma_4\\ \gamma_5\\ \gamma_6\end{bmatrix} = \begin{bmatrix}S_{11} & S_{12} & S_{13} & 0 & 0 & 0\\ S_{21} & S_{22} & S_{23} & 0 & 0 & 0\\ S_{31} & S_{32} & S_{33} & 0 & 0 & 0\\ 0 & 0 & 0 & S_{44} & 0 & 0\\ 0 & 0 & 0 & 0 & S_{55} & 0\\ 0 & 0 & 0 & 0 & 0 & S_{66}\end{bmatrix}\begin{bmatrix}\sigma_1\\ \sigma_2\\ \sigma_3\\ \tau_4\\ \tau_5\\ \tau_6\end{bmatrix} \quad (2)$$

No coupling exists between normal stresses $\sigma_1, \sigma_2, \sigma_3$ and shear strains $\gamma_4, \gamma_5, \gamma_6$ that are, normal stresses acting along principal material direction produce only normal strain and no coupling exists between shear τ_4, τ_5, τ_6 and normal strain $\varepsilon_1, \varepsilon_2, \varepsilon_3$ that is, shear stresses acting on principal material planes produce only shear strains. No coupling exists between shear stress acting on one plane and a shear strain on a different plane; that is shear stress acting on a principal plane produces a shear strain only on that plane. If an orthotropic material element is subjected to uniaxial tensile loading in the longitudinal direction, σ_1, then from the above equation

$$\varepsilon_1 = S_{11}\sigma_1 \quad (3)$$

$$\varepsilon_2 = S_{12}\sigma_1 \quad (4)$$

$$\varepsilon_3 = S_{13}\sigma_1 \quad (5)$$

$$\gamma_4 = \gamma_5 = \gamma_6 = 0 \quad (6)$$

From engineering considerations we have, $\varepsilon_1 = \frac{\sigma_1}{E_1}$

$$\varepsilon_2 = -\frac{v_{12}}{E_1}\sigma_1 \quad (7)$$

$$\varepsilon_3 = -\frac{v_{13}}{E_1}\sigma_1 \quad (8)$$

$$\gamma_4 = \gamma_5 = \gamma_6 = 0 \quad (9)$$

Recall that the first and second subscripts in Poisson's ratio denote stress and strain directions, respectively from above equation we obtain the relations as

$$S_{11} = \frac{1}{E_1}S_{12} = -\frac{v_{12}}{E_1}S_{13} = -\frac{v_{13}}{E_1} \quad (10)$$

If a material element is subjected to uniaxial tensile loading σ_2 in the in-plane transverse direction, we have in a similar fashion

$$\varepsilon_1 = S_{12}\sigma_2 = -\frac{v_{21}}{E_2}\sigma_2 \quad (11)$$

$$\varepsilon_2 = S_{22}\sigma_2 = \frac{\sigma_2}{E_2} \quad (12)$$

$$\varepsilon_3 = S_{23}\sigma_2 = -\frac{v_{23}}{E_2}\sigma_2 \quad (13)$$

$$\gamma_4 = \gamma_5 = \gamma_6 = 0 \quad (14)$$

From which we obtain the relations, $S_{12} = -\frac{v_{21}}{E_1}S_{22} = \frac{1}{E_2}S_{13} = -\frac{v_{23}}{E_2}$

Uniaxial normal loading σ_3 in the out of the plane transverse direction yields

$$\varepsilon_1 = S_{13}\sigma_3 = -\frac{v_{31}}{E_3}\sigma_3 \quad \textbf{(15)}$$

$$\varepsilon_2 = S_{23}\sigma_3 = -\frac{v_{32}}{E_3}\sigma_3 \quad \textbf{(16)}$$

$$\varepsilon_3 = S_{33}\sigma_3 = \frac{\sigma_3}{E_3} \quad \textbf{(17)}$$

From which we obtain the relations, $S_{13} = -\frac{v_{31}}{E_3} S_{33} = \frac{1}{E_3} S_{23} = -\frac{v_{32}}{E_3}$

In-plane pure shear loading, τ_6, yield $\varepsilon_1 = \varepsilon_2 = \varepsilon_3 = \gamma_4 = \gamma_5 = 0$, $\gamma_6 = S_{66}\tau_6 = \frac{\tau_6}{G_{12}}$

From which we obtain, $S_{66} = \frac{1}{G_{12}}$

Out of plane pure shear loading τ_4 on the 2-3 plane yield $\varepsilon_1 = \varepsilon_2 = \varepsilon_3 = \gamma_4 = \gamma_5 = 0$, $\gamma_4 = S_{44}\tau_4 = \frac{\tau_4}{G_{23}}$

From which we obtain, $S_{44} = \frac{1}{G_{23}}$

Finally, out-of*plane pure shear loading τ_5 on the 1-3 plane yields $\varepsilon_1 = \varepsilon_2 = \varepsilon_3 = \gamma_4 = \gamma_5 = 0$, $\gamma_5 = S_{55}\tau_5 = \frac{\tau_5}{G_{13}}$

From which we obtain, $S_{55} = \frac{1}{G_{13}}$

The stress-strain relations can be then be expressed in terms of engineering constants as follows

$$\begin{bmatrix}\sigma_1\\ \sigma_2\\ \sigma_3\\ \tau_4\\ \tau_5\\ \tau_6\end{bmatrix} = \begin{bmatrix} \frac{1}{E_1} & -\frac{v_{21}}{E_2} & -\frac{v_{31}}{E_3} & 0 & 0 & 0 \\ -\frac{v_{12}}{E_1} & \frac{1}{E_2} & -\frac{v_{32}}{E_3} & 0 & 0 & 0 \\ -\frac{v_{13}}{E_1} & -\frac{v_{23}}{E_2} & \frac{1}{E_3} & 0 & 0 & 0 \\ 0 & 0 & 0 & \frac{1}{G_{23}} & 0 & 0 \\ 0 & 0 & 0 & 0 & \frac{1}{G_{13}} & 0 \\ 0 & 0 & 0 & 0 & 0 & \frac{1}{G_{12}} \end{bmatrix} \begin{bmatrix}\varepsilon_1\\ \varepsilon_2\\ \varepsilon_3\\ \gamma_4\\ \gamma_5\\ \gamma_6\end{bmatrix} \quad \textbf{(18)}$$

Matrix notation:

$$\begin{aligned} \epsilon_1 &= \epsilon_{11}\epsilon_4 = \gamma_{23}\sigma_1 = \sigma_{11}\sigma_4 = \sigma_{23} \\ \epsilon_2 &= \epsilon_{22}\epsilon_5 = \gamma_{13}\sigma_3 = \sigma_{33}\sigma_5 = \sigma_{13} \\ \epsilon_3 &= \epsilon_{33}\epsilon_6 = \gamma_{12}\sigma_3 = \sigma_{33}\sigma_6 = \sigma_{12} \end{aligned} \quad \textbf{(19)}$$

In-plane ($x_1 - x_2$): 4 independent elastic constants: $E_1 E_2 \vartheta_{12} G_{12}$

And compliance matrix symmetric $-\frac{v_{12}}{E_1} = -\frac{v_{21}}{E_2}$

Notation for Poisson's ratio: $\vartheta_{ij} = -\frac{\epsilon_j}{\epsilon_i}$

Unit cell: In the x_1 direction, length of unit cell is 2lcos θ

In the x_2 direction, length of unit cell is h $+$ lcos θ

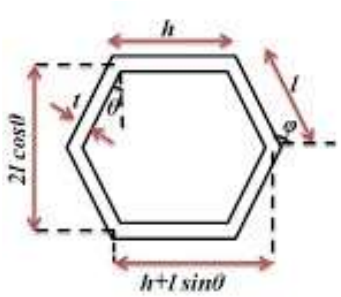

Fig.1.

Young's modulus $= \frac{\text{stress in one direction}}{\text{strain in the one direction}} = \frac{\sigma_1}{\epsilon_1}$

Stress in one direction $= \frac{\text{load}}{\text{length} \times \text{depth}}$

Load $= P$

Length $= h + lsin\theta$

Depth $= b$

$$\sigma_1 = \frac{P}{\mathrm{h} + \mathrm{lsin\theta b}} \tag{20}$$

Strain in one direction $= \frac{\text{deformation in one direction}}{\text{unit cell length}}$

Deformation in one direction $= \delta sin\theta$

Unit cell length $= lcos\theta$

$$\epsilon_1 = \frac{\delta sin\theta}{lcos\theta} \tag{21}$$

We should relate load P to the deformation δ to get the stiffness of the cell

Bending moment:

Bending moment will be $[^{-ve}]$. If they have tension on the top.

Bending moment will be $[^{+ve}]$. If they have tension on the bottom.

$$M_B - M_A = \int_A^B \mathrm{V\ dV} \tag{22}$$

$[M_B - M_A]$ is the integral of the shear diagram or v diagram between the two pairs.

For honeycomb when we connect two cantilever of length l_{12}

$$\delta = 2 \times \frac{FL^3}{3EI} \tag{23}$$

F $=$ Force

L $= \frac{l}{2}$

E $=$ ES

I $= \frac{bt^3}{12}$

$$\delta = \frac{2 \times P sin\theta \left[{}^{l}/_{2}\right]^{3}}{3E_s I} \quad (24)$$

$$= \frac{2 \times P sin\theta \ \frac{l^3}{4}}{3E_s I}$$

$$\delta = \frac{P sin\theta \ l^3}{12E_s I}$$

Combining $E_1^* =$ Young's modules in the one direction

$$E_1^* = \frac{\sigma_1}{\epsilon_1} \quad (25)$$

We have

$$\left[\sigma_1 = \frac{P}{\mathrm{h+lsin\theta b}} \ , \ \epsilon_1 = \frac{\delta sin\theta}{lcos\theta}\right],$$

$$= \frac{P}{\frac{\mathrm{h+lsin\theta b}}{\frac{\delta sin\theta}{lcos\theta}}} \quad (26)$$

We have

$$\left[\delta = \frac{P sin\theta \ l^3}{12E_s I} \ , \ \mathrm{I} = \frac{bt^3}{12}\right]$$

$$= \frac{P}{\mathrm{h + lsin\theta b}} \times \frac{lcos\theta}{P sin\theta \ l^3}$$

$$= E_s \left[\frac{t}{l}\right]^3 \frac{lcos\theta}{[\mathrm{h + lsin\theta b}]sin^2\theta}$$

$$E_1^* = E_s \left[\frac{t}{l}\right]^3 \frac{lcos\theta}{[\frac{\mathrm{h}}{\mathrm{l}} + \mathrm{sin\theta}]sin^2\theta} \quad (27)$$

III. POISSON'S RATIO

Loading in X_1 direction

$$\gamma_{12}^* = -\frac{\epsilon_2}{\epsilon_1} \quad (28)$$

We have

$$\left[\epsilon_1 = -\frac{\delta sin\theta}{lcos\theta} \ \epsilon_2 = \frac{\delta cos\theta}{h+lsin\theta}\right]$$

$$= \frac{\frac{\delta cos\theta}{h + lsin\theta}}{\frac{\delta sin\theta}{lcos\theta}}$$

$$= \frac{lcos^2\theta}{[h + lsin\theta]sin\theta}$$

$$\gamma_{12}^* = \frac{cos^2\theta}{\left[\frac{h}{l} + sin\theta\right]sin\theta} \quad (29)$$

Poisson's ratio only depends on the cell geometry

A. Elastic Buckling

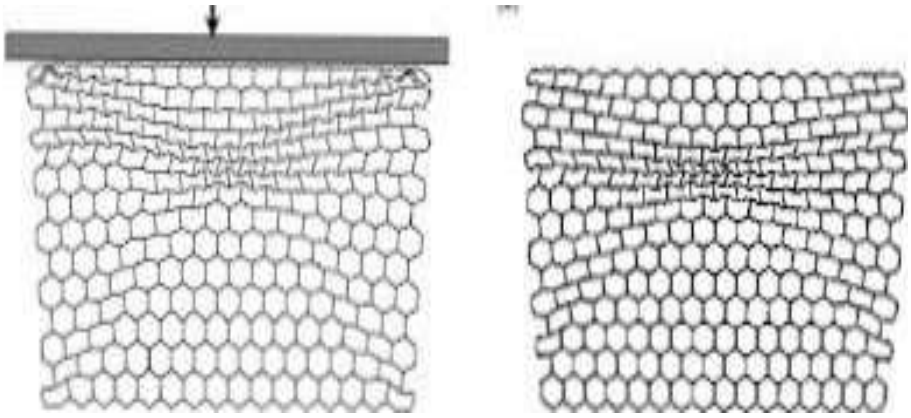

Fig.2.

Cell collapse by buckling of walls of length h when loaded in X_2 direction. No buckling for (σ_1), bending of inclined cell goes to densification. So we have (σ_{el}^*)

$$[\sigma_{el}^*] = \frac{P_{cr}}{2lcos\theta b} \quad \textbf{(30)}$$

We have

$$P_{cr} = \frac{n^2\pi^2 E_s I}{h^2} = \frac{\frac{n^2\pi^2 E_s I}{h^2}}{2lcos\theta b} = \frac{n^2\pi^2 E_s I}{h(2lcos\theta)b} \quad \textbf{(31)}$$

We have

$$I = \frac{bt^3}{12}$$

$$[\sigma_{el}^*] = \frac{n^2\pi^2 E_s I}{h(2lcos\theta)b} \times \frac{bt^3}{12}$$

$$[\sigma_{el}^*] = \frac{n^2\pi^2}{24} E_s \frac{\left[\frac{t}{l}\right]^3}{\left[\frac{h}{l}\right]^2 cos\theta} \quad \textbf{(32)}$$

IV. PLASTIC COLLAPSE STRESS

Internal moment at formation of plastic hinge, plastic moment M_p

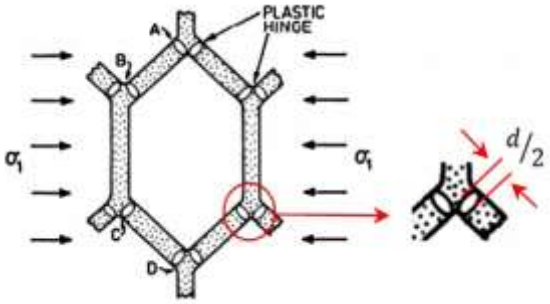

Fig.3.

$$M_p = [\sigma_{ys} b\, t/2]\left(\frac{t}{2}\right) \quad \textbf{(33)}$$

$$M_p = \left[\sigma_{ys}\frac{bt^2}{4}\right] \quad \textbf{(34)}$$

Applied moment from applied stress

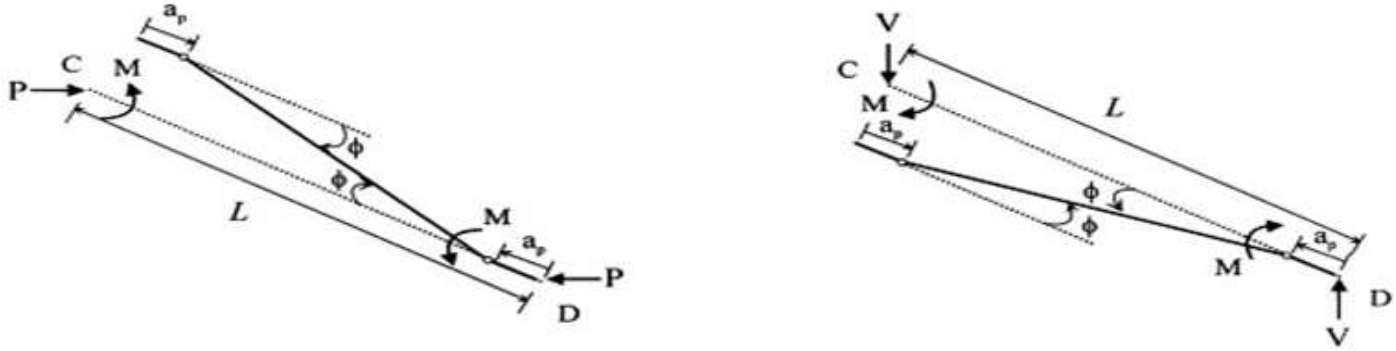

Fig.4.

$$2M_{ap} - Plsin\theta = 0$$

$$2\,M_{ap} = Plsin\theta \quad \textbf{(35)}$$

$$M_{ap} = \frac{Plsin\theta}{2} \quad \textbf{(36)}$$

We have

$$M_{ap} = \sigma_1[h + lsin\theta]\,b\frac{lsin\theta}{2}$$

$$\sigma_1[h + lsin\theta]\,b\frac{lsin\theta}{2} = \frac{Plsin\theta}{2}$$

$$\sigma_1 = \frac{P}{[h + lsin\theta]\,b} \quad \textbf{(37)}$$

Plastic collapse of honeycomb at $[\sigma_{pl}^{*}]$, when

$$M_{ap} = M_{pl}$$

$$(\sigma_{pl}^{*})[h + lsin\theta]\,b\,\frac{lsin\theta}{2} = \sigma_{ys}\frac{bt^2}{4}$$

$$(\sigma_{pl}^{*}) = \sigma_{ys}\left[\frac{t}{l}\right]^2\frac{1}{2[h + lsin\theta]sin\theta}$$

$$(\sigma_{pl}^{*}) = \sigma_{ys}\frac{\left[\frac{t}{l}\right]^2}{2[h + lsin\theta]sin\theta} \quad \textbf{(38)}$$

In the above equation we have

$$2M_p - Plsin\theta = 0$$

$$2M_p = Plsin\theta \quad \textbf{(39)}$$

The moment arm l is reduced to $\left[l - \frac{t}{l}\right]$

$$2M_p = P\left[l - \frac{t}{l}\right]sin\theta$$

$$2\left[\frac{b\sigma_y d^2}{2(n+2)}\right] = \sigma_p(h + lsin\theta)\,b\left[l - \frac{t}{l}\right]sin\theta$$

$$= \sigma_p\frac{2\left[\frac{b\sigma_y\left[\frac{t}{l}\right]^2}{2(n+2)}\right]}{(h + lsin\theta)\,b\left[l - \frac{t}{l}\right]sin\theta}$$

$$\sigma_p = \left[\frac{\sigma_y}{n+2}\frac{\left[\frac{t}{l}\right]^2}{(h+l\sin\theta)b\left[l-\frac{t}{l}\right]\sin\theta}\right] \quad \textbf{(40)}$$

The corresponding locking strain based on relative density can be calculated as variables affecting honeycomb mechanical properties is

V. RELATIVE DENSITY

$$\frac{\rho^*}{\rho_s} = \frac{\frac{M_s}{v_t}}{\frac{M_s}{v_s}}$$

$$\frac{\rho^*}{\rho_s} = \frac{v_s}{v_t} \quad \textbf{(41)}$$

If the relative density $\left[\frac{\rho^*}{\rho_s}\right]$ increases you will get more materials on the cell edges and volume decreases. If the relative density $\left[\frac{\rho^*}{\rho_s}\right]$ is limited you will get isolated pores in the solid surface. We have the relative density

$$\frac{\rho^*}{\rho_s} = \frac{\left[\frac{t}{l}\right]\left[\frac{h}{l}+2\right]}{2cos\theta\left[\frac{h}{l}+sin\theta\right]}$$

$$\rho^* = \frac{\left[\frac{t}{l}\right]\left[\frac{h}{l}+2\right]}{2cos\theta\left[\frac{h}{l}+sin\theta\right]} \quad \textbf{(42)}$$

The porosity which in fact is the pore volume is $1-\rho^*$.The volume is approximately equal to the locking strain ε_d

$$\varepsilon_d = 1 - \frac{\left[\frac{t}{l}\right]\left[\frac{h}{l}+2\right]}{2cos\theta\left[\frac{h}{l}+sin\theta\right]} \quad \textbf{(43)}$$

The equation of strain energy is

$$U = \int[\int \sigma d\varepsilon]\, dv \quad \textbf{(44)}$$

Since the thickness of the cell wall is changing the 'U' presented above can only capture the response of individual rows. Therefore considering $[\sigma = \sigma_p]\&[\varepsilon = \varepsilon_d]$ Stress to plateau stress & strain to locking strain. Strain energy per unit volume would be

$$U = \sum_{i=1}^{6} \sigma_{pi}\varepsilon_{di} \quad \textbf{(45)}$$

Based on the obtained equation the strain energy for the entire structure can be obtained as

$$U = \int[\int \sigma d\varepsilon]\, dv$$

$$U = AL\sum_{i=1}^{6}\sigma_{pi}\frac{\varepsilon_{di}}{6}$$

$$A = 2blcos\theta \;,\; L = 15C + 16lsin\theta \quad \textbf{(46)}$$

VI. STRAIN ENERGY

$$U = (2blcos\theta)(15C + 16lsin\theta)\sum_{i=1}^{6}\sigma_{pi}\frac{\varepsilon_{di}}{6} \quad \textbf{(47)}$$

Where σ_p is calculated for power hardening model as

$$\sigma_p = \left[\frac{\sigma_y}{n+2}\frac{\left[\frac{t}{l}\right]^2}{(h+l\sin\theta)b\left[l-\frac{t}{l}\right]\sin\theta}\right] \quad \textbf{(48)}$$

The cell volume and mass are

$$V_c = db[4l+2c]$$

$$m_c = \rho_s db[4l+2c] \quad \textbf{(49)}$$

The mass of the entire structure is

$$M = \rho_s b(32l + 23c) \sum_{i=1}^{6} d_i \quad \textbf{(50)}$$

Energy absorption:
Energy absorption of the structure is

$$e_{ab} = \frac{U}{M}$$

$$e_{ab} = \frac{(2b l\cos\theta)(15C + 16l\sin\theta) \sum_{i=1}^{6} \sigma_{pi} \frac{\varepsilon_{di}}{6}}{\rho_s b(32l + 23c) \sum_{i=1}^{6} d_i} \quad \textbf{(51)}$$

VII. NUMERICAL ANALYSIS

C (mm)	L (mm)	B (mm)	D(t) (mm)
5	5	20	1

A numerical analysis is conducted to the honeycomb structure by the given values

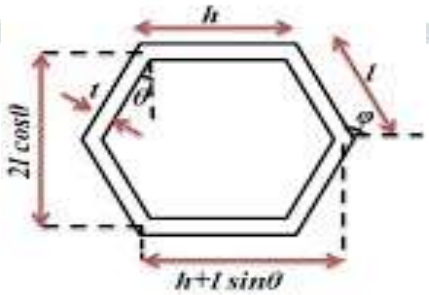

Fig.5.

The geometry of each cell is same in the given honeycomb structure. So taking single cell in to consideration, the value of cell are given below 5mm for the cell horizontal wall size, 5mm for the inclined wall size, 20mm is the depth of the cell and thickness of the cell is 1mm. The angle of the cell is 30º, θ is the angle of the cell. In order to validate the obtained analytical equations and comparing the result of equations, energy absorption of honeycomb structures made of angles of the cell from (25° to 40°) and also the thickness of the cell from (1mm to 2mm) Is simulated in MATLAB.

VIII. ENERGY ABSORPTION WITH DIFFERENT ANGLES

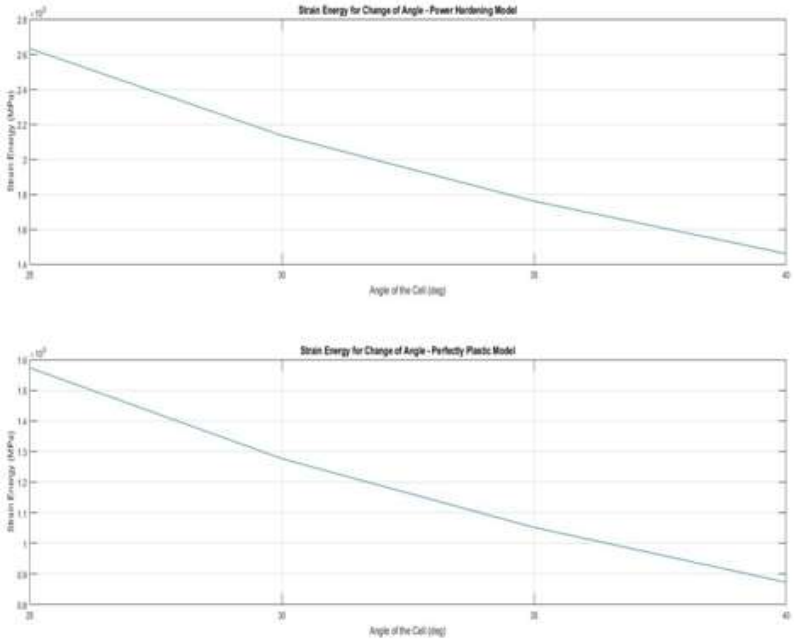

Fig.6.

The above graph shows the energy absorption of the honeycomb structure under loading with different angles from (25° to 40°). This MATLAB simulation is done for two different models which is power hardening model and perfectly plastic model.

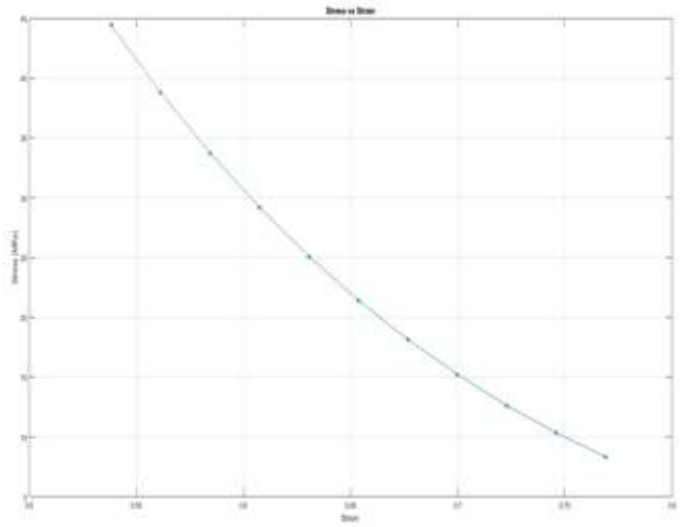

Fig.7.

By comparing the above two graph which is power hardening model and perfectly plastic model the stress strain graph is plotted.

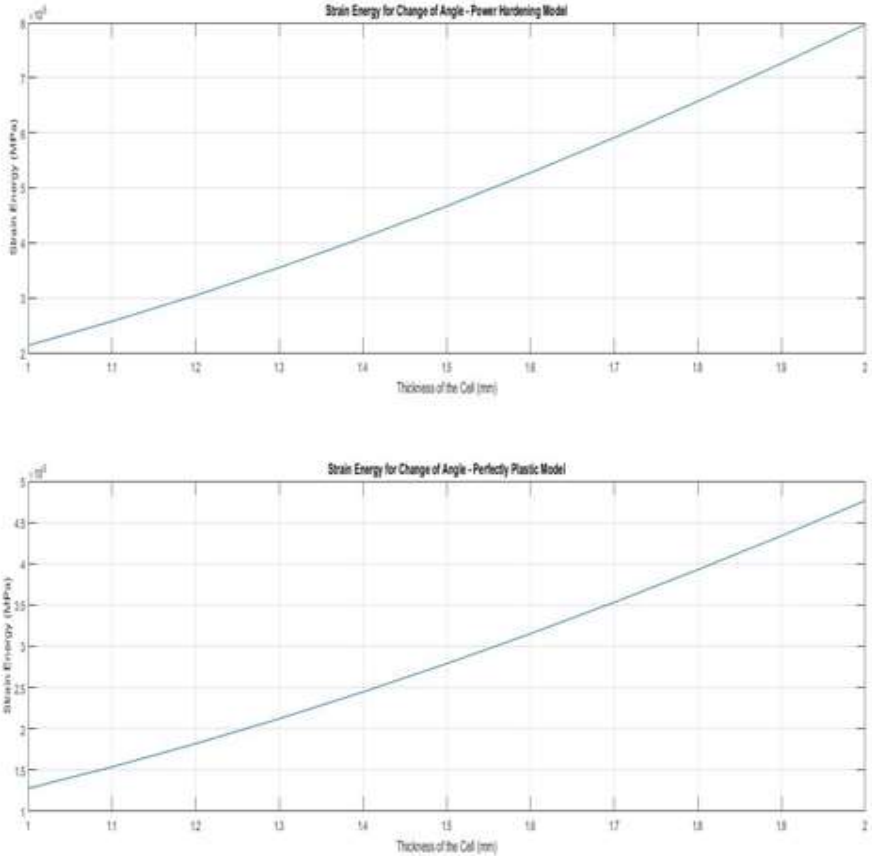

Fig.8.

The above graph shows the energy absorption of the honeycomb structure under loading with different thickness of the cell from (1mm to 2mm). This MATLAB simulation is done for two different models which is power hardening model and perfectly plastic model.

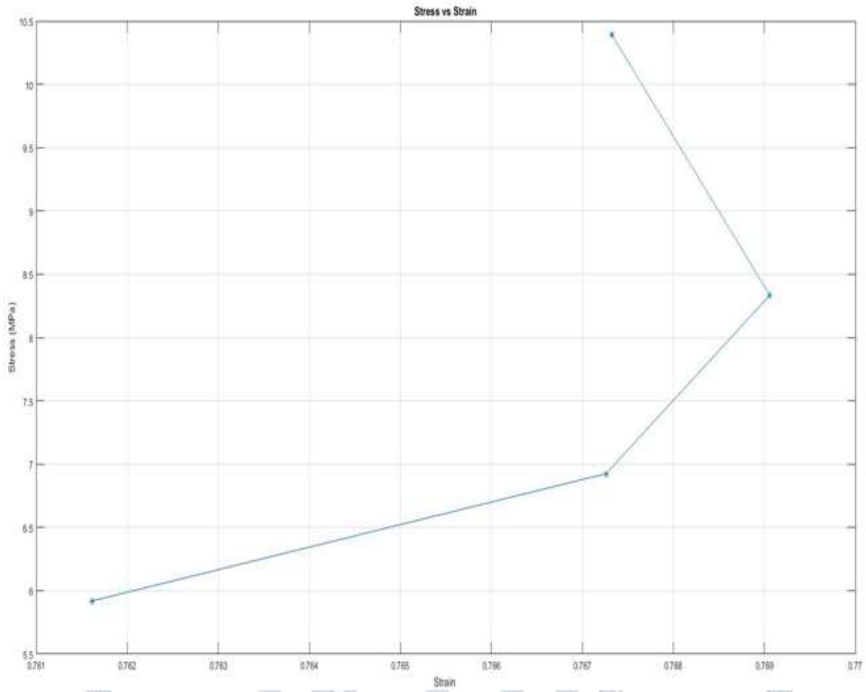

Fig.9.

IX. ANSYS SIMULATION

In order to validate the numerical simulation method in MATLAB software, a test has been conducted in Ansys software as the falling a weight with low velocity on a honeycomb structure. Our model is a 6061-O aluminum honeycomb structure. This structure has 6 rows with different thicknesses and angles.

TABLE I:

Object Name	**Geometry**
State	Fully Defined
Definition	
Source	Athulajayan
Type	Step
Length Unit	Meters
Element Control	Program Controlled
Display Style	Body Color
Bounding Box	
Length X	20. mm
Length Y	52.5 mm
Length Z	118. mm
Properties	
Volume	32458 mm³
Mass	0.2548 kg
Scale Factor Value	1.
Statistics	
Bodies	1
Active Bodies	1
Nodes	24919
Elements	3808
Mesh Metric	None
Basic Geometry Options	

TABLE II:

Material	
Assignment	Structural Steel
Nonlinear Effects	Yes
Thermal Strain Effects	Yes
Bounding Box	
Length X	20. mm
Length Y	52.5 mm
Length Z	118. mm
Properties	
Volume	32458 mm³
Mass	0.2548 kg
Centroid X	-2.1747e-015 mm
Centroid Y	11.248 mm
Centroid Z	58.053 mm
Moment of Inertia Ip1	395.53 kg·mm²
Moment of Inertia Ip2	331.49 kg·mm²
Moment of Inertia Ip3	81.027 kg·mm²
Statistics	
Nodes	24919
Elements	3808
Mesh Metric	None

TABLE III:

Solid Bodies	Yes
Surface Bodies	Yes
Line Bodies	No
Parameters	Independent
Parameter Key	ANS;DS
Attributes	No
Named Selections	No
Material Properties	No
Advanced Geometry Options	
Use Associativity	Yes
Coordinate Systems	No
Reader Mode Saves Updated File	No
Use Instances	Yes
Smart CAD Update	Yes
Compare Parts On Update	No
Attach File Via Temp File	Yes
Temporary Directory	D:\ansys examples
Analysis Type	3-D
Mixed Import Resolution	None
Decompose Disjoint Geometry	Yes
Enclosure and Symmetry Processing	Yes

TABLE V: Model (A4, B4, C4) > Static Structural 3 (C5) > Solution (C6) > Equivalent Stress

Time [s]	Minimum [MPa]	Maximum [MPa]
1.	1.2202e-002	26.779
2.	2.4405e-002	53.558
3.	3.6607e-002	80.336
4.	4.881e-002	107.12
5.	6.1012e-002	133.89
6.	7.3215e-002	160.67
7.	8.5417e-002	187.45
8.	9.762e-002	214.23
9.	0.10982	241.01
10.	0.12202	267.79

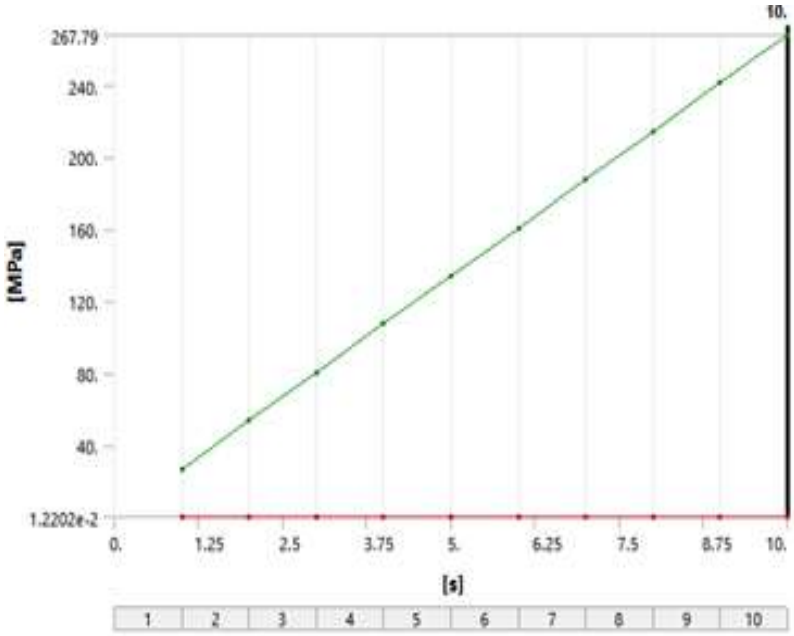
10.
267.79
240.
200.
160.
120.
80.
40.
1.2202e-2
[MPa]
0.
1.25
2.5
3.75
5.
6.25
7.5
8.75
10.
[s]
1
2
3
4
5
6
7
8
9
10

Fig.10.

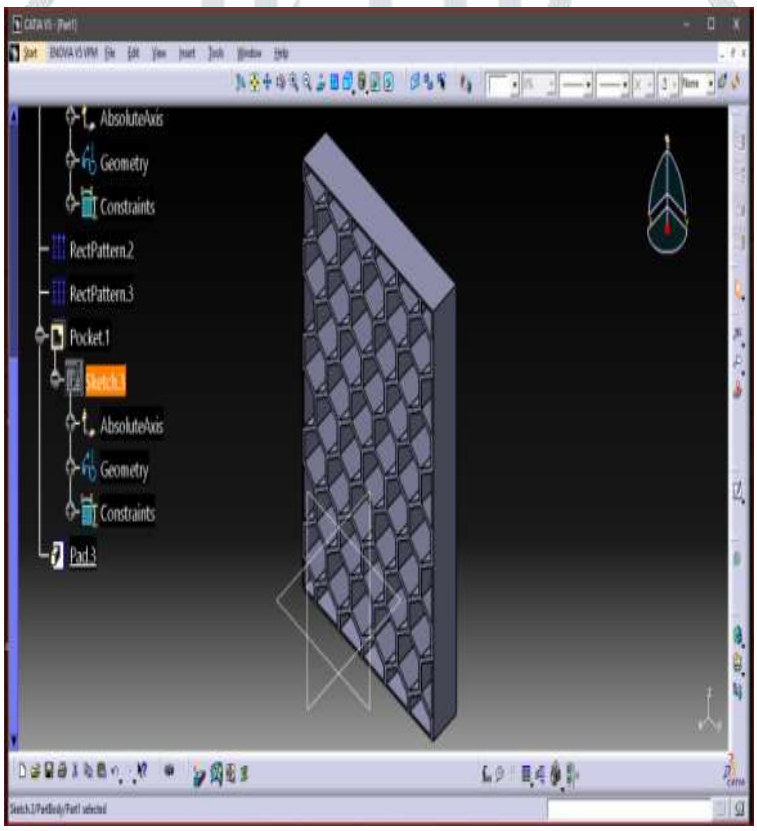
AbsoluteAxis
Geometry
Constraints
RectPattern.2
RectPattern.3
Pocket.1
Sketch.3
AbsoluteAxis
Geometry
Constraints
Pad.3

Fig.11.

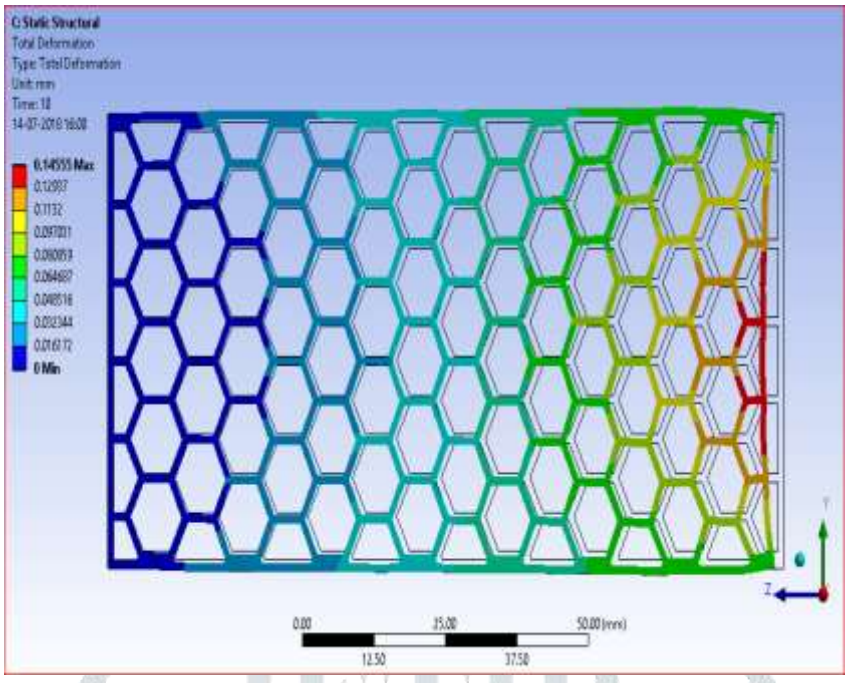

Fig.12.

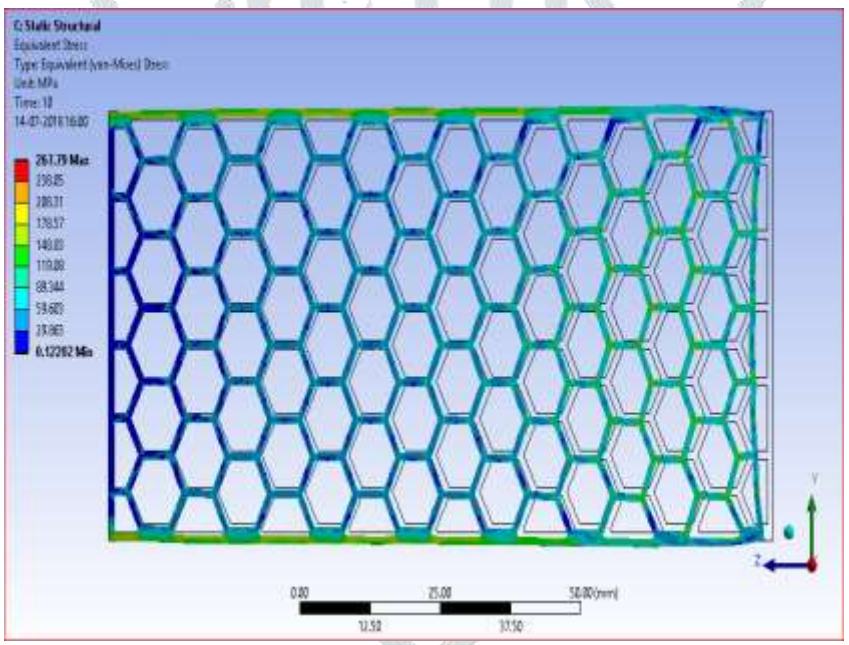

Fig.13.

TABLE VI: Structural Steel > Constants

Density	7.85e-006 kg mm^-3
Isotropic Secant Coefficient of Thermal Expansion	1.2e-005 C^-1
Specific Heat	4.34e+005 mJ kg^-1 C^-1
Isotropic Thermal Conductivity	6.05e-002 W mm^-1 C^-1
Isotropic Resistivity	1.7e-004 ohm mm

TABLE VII: Structural Steel > Appearance

Red	Green	Blue
132	139	179

TABLE VIII: Structural Steel > Compressive Ultimate Strength

Compressive Ultimate Strength MPa
0

TABLE IX: Structural Steel > Compressive Yield Strength

Compressive Yield Strength MPa
250

TABLE X: Structural Steel > Tensile Yield Strength

Tensile Yield Strength MPa
250

TABLE XI: Structural Steel > Tensile Ultimate Strength

Tensile Ultimate Strength MPa
460

TABLE XII: Structural Steel > Isotropic Secant Coefficient of Thermal Expansion

Zero-Thermal-Strain Reference Temperature C
22

TABLE XIII: Structural Steel > Alternating Stress Mean Stress

Alternating Stress MPa	Cycles	Mean Stress MPa
3999	10	0
2827	20	0
1896	50	0
1413	100	0
1069	200	0
1069	200	0
441	2000	0
262	10000	0
214	20000	0
138	1.e+005	0
114	2.e+005	0
86.2	1.e+006	0

TABLE XIV: Structural Steel > Strain-Life Parameters

Strength Coefficient MPa	Strength Exponent	Ductility Coefficient	Ductility Exponent	Cyclic Strength Coefficient MPa	Cyclic Strain Hardening Exponent
920	-0.106	0.213	-0.47	1000	0.2

TABLE XV: Structural Steel > Isotropic Elasticity

Temperature C	Young's Modulus MPa	Poisson's Ratio	Bulk Modulus MPa	Shear Modulus MPa
	2.e+005	0.3	1.6667e+005	76923

TABLE XVI: Structural Steel > Isotropic Relative Permeability

Relative Permeability
10000

Nomenclature:

P = load

$\frac{t}{l}$ = Relative density

v_t = Total volume

h= length

M_s = Mass of solid

b= depth

$\frac{h}{l}$, θ = cell geometry

σ =Stress

γ^* = Poisson's ratio

ϵ =Strain

σ^* = plateau stress

F = force

el = elastic buckling

I = moment of inertia

P_{cr} = Buckling in critical

E_s = Modules of solid

n = end constrained factor

E^* = Young's modules

v_s = Volume of solid

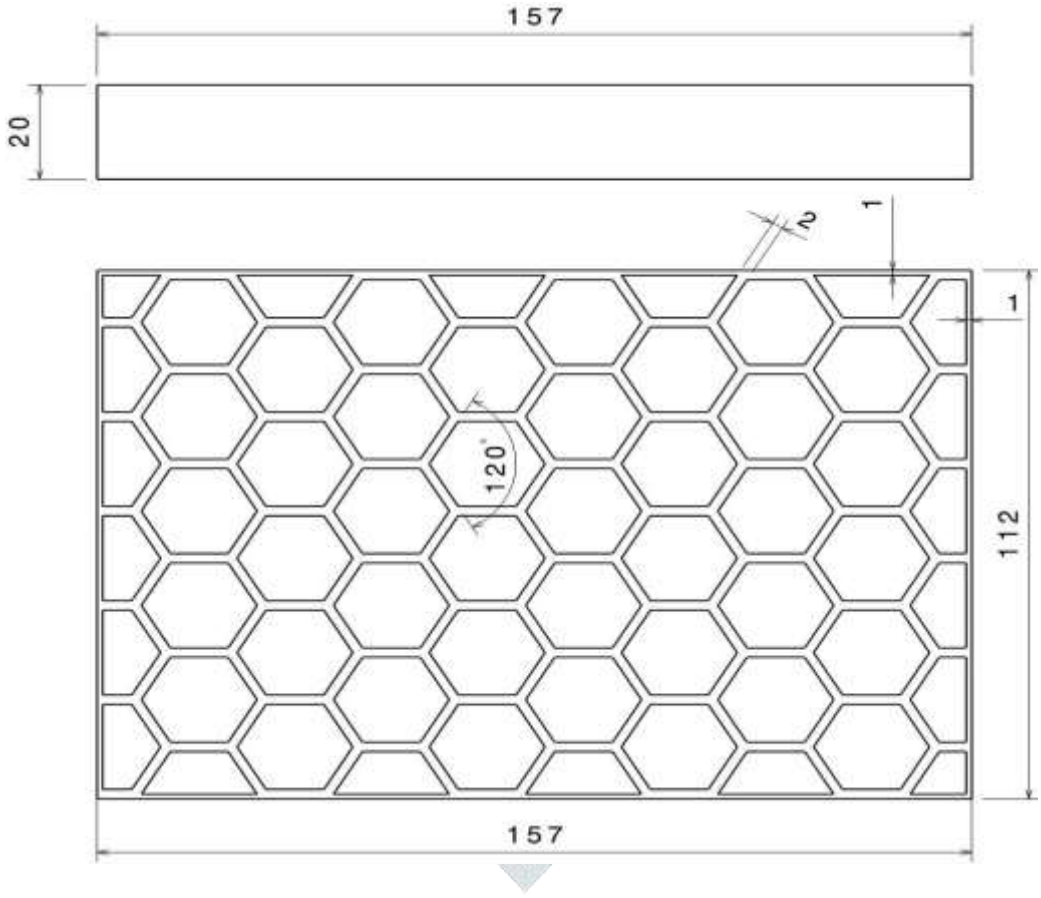

Fig.14.

X. CONCLUSION

The obtained stress and locking strain values is used to derive the energy absorption capacity of a honeycomb structure under loading. To validate the compression strength of the honeycomb structure, a finite element analysis on the absorption capacity was performed in this research. After comparing the deflection in the honeycomb structure with different angles,[30]^° has very less deflection when compared to other angles and in different thickness, 2mm thickness has very less deflection. In this research the numerical results of energy absorption model is giving more appropriate values when compared to plastic model. Comparison shows that the obtained analytical results are acceptable accordance with simulation result in ANSYS software. The maximum error between the numerical results and simulation results is 10-20%. The structure with in-plane loading reduces the physical damage compared to the out-plane loading. The finite element method is the most effective method of numerical calculations in the structural analysis.

XI. REFERENCE

[1]Ariel stocchi and Lucas colabella, "Manufacturing and testing of a sandwich panel honeycomb core reinforced with natural fiber fabrics", (2013).

[2]JabihullaShariffMd and K.SudhirChakravarthy,"Comparison of Tensile Strength with Experimental and Numerical Analysis of a Sandwich Panel of Rhombus and Hexagonal Honeycomb Core Structures", (2016).

[3]Dipak G and Vamja, GG. Tejani, "Experimental Test on Sandwich Panel Composite Material", International Journal of Innovative Research in Science, (2013).
[4]ZoranPetrovic and Ivan Lazarevic, "Design and analysis of the flat honeycomb sandwich structure" (2015
[5]David Griese, "Finite Element Modeling and Design of Honeycomb Sandwich Panels for Acoustic Performance",(2012).
[6]J.L. Mantari and A.S. Oktem, C. GuedesSoares, "A new trigonometric shear deformation theory for isotropic, laminated composite and sandwich plates",International Journal of Solids and Structures, (2011).
[7]S., Wang and Sha, Y,Shi. H, " Analysis of isotropic, sandwich and laminated plates by a meshless method and various shear deformation theories", (2009).
[8]Murat Yazicia and Jefferson Wright b ,ArunShukla, "Experimental and numerical study of foam filled corrugated core steel sandwich structures subjected to blast loading",(2013).
[9]Avachat S and Zhou M, " Effect of face sheet thickness on dynamic response of composite sandwich plates to underwater impulsive loading", (2012).
[10]Tao Fan and Guanpingzou, "Influences of defects on dynamic crushing properties of functionally graded honeycomb structures", (2014).
[11]Jianxiong and LiMa,Linzhi, "Mechanical behavior of sandwich panels with hollow Al–Si tubes core construction", (2016)
[12]RecepGunes and Kemal Arslan, M. Kemal Apalak, J.N. Reddy, "Numerical Investigations on the Ballistic Performance of Honeycomb Sandwich Structures Reinforced by Functionally Graded Plates", (2014).
[13]K R Mangipudi and S W van Buuren, "The microstructural origin of strain hardening in two-dimensional open-cell metal foams", (2010).
[14]A Honig and W J Stronge, "In-plane dynamic crushing of honeycomb crush band initiation and wave trapping", (2002).
[15]L L Hu and T X Yu, Z Y Gao, "The inhomogeneous deformation of polycarbonate circular honeycombs under in-plane compression", (2008).
[16]B Hou and H Zhao, S Pattofatto, "Inertia effects on the progressive crushing of aluminum honeycombs under impact loading" (2012).
[17]Hong and S.T. Pan, J., Tyan, T. and Prasad, "Quasi-static Crush Behavior of AluminumHoneycomb Specimens under Compression Dominant Combined Loads", (2006).
[18]S. Heimbs& P. Middendorf& S. Kilchert& A. F. Johnson &M. Maier, "Experimental and Numerical Analysis of Composite Folded Sandwich Core Structures Under Compression", (2007).
[19]G.A.O.Davies, D.Hitchings, T. Besant, A. Clarke, C. Morgan, "Compression after impact strength of composite sandwich panels", Composites Science and Technology, (2009).
[20]JabihullaShariffMd, "Design Modulation of Composite Material Sandwich Panels with Different Inner Polyethylene Core Structures" International Journal of Engineering Research & Technology, (2014).
[21]Ch.Naresh, A. Gopi Chand, K.SunilRatna Kumar, P.S.B.Chowdary, "Numerical Investigation into Effect of Cell Shape on the Behavior of Honeycomb Sandwich Panel", International Journal of Innovative Research in Science, (2013).
[22]SalihN.Akour, Hussein Z.Maaitah, "Effect of Core Material Stiffness on Sandwich Panel Behaviour Beyond the Yield Limit", (2010).
[23]M. Meo, R. Vignjevic, G. Marengo, "The response of honeycomb sandwich panels under low-velocity impact loading", International Journal of Mechanical Sciences, (2005).
[24]Ahmed Abbadi, Y. Koutsawa, A. Carmasol, S. Belouettar, Z. Azarib, "Experimental and numerical characterization of honeycomb sandwich composite panels", (2009).
[25]K.KanthaRao, K. JayathirthaRao, A.G.Sarwade, B.MadhavaVarma,"Bending Behavior of Aluminum Honey Comb Sandwich Panels", International Journal of Engineering and Advanced Technology, (2012).